Communication

Diode or Tunnel-Diode Characteristics? Resolving the Catalytic Consequences of Proton Coupled Electron Transfer in a Multi-Centered Oxidoreductase

James D. Gwyer, David J. Richardson, and Julea N. Butt

J. Am. Chem. Soc., **2005**, 127 (43), 14964-14965• DOI: 10.1021/ja054160s • Publication Date (Web): 05 October 2005

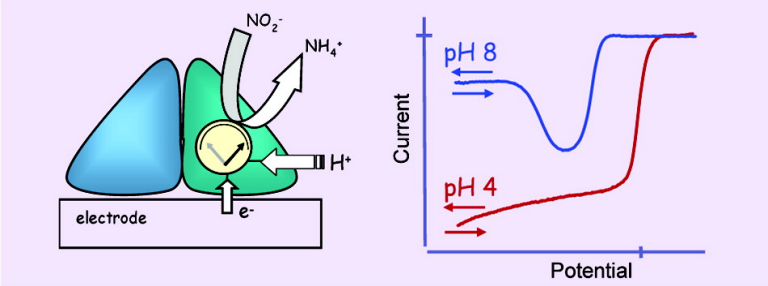

More About This Article

Additional resources and features associated with this article are available within the HTML version:

- Supporting Information
- Links to the 6 articles that cite this article, as of the time of this article download
- Access to high resolution figures
- Links to articles and content related to this article
- Copyright permission to reproduce figures and/or text from this article

View the Full Text HTML

J|A|C|S
COMMUNICATIONS

Published on Web 10/05/2005

Diode or Tunnel-Diode Characteristics? Resolving the Catalytic Consequences of Proton Coupled Electron Transfer in a Multi-Centered Oxidoreductase

James D. Gwyer, David J. Richardson, and Julea N. Butt*

Centre for Metalloprotein Spectroscopy and Biology, School of Chemical Sciences and Pharmacy, School of Biological Sciences, University of East Anglia, Norwich, NR4 7TJ, U.K.

Received June 23, 2005; E-mail: j.butt@uea.ac.uk

More than a third of known enzymes are oxidoreductases, and of these, many possess multiple redox active centers. These centers are positioned to form chains that relay electrons between "active" sites where intermolecular electron transfer results in the oxidation and compensating reduction of selected redox partners.[1] The proximity of neighboring relay stations, typically <14 Å, suggests that even relatively endergonic electron tunneling between these centers will occur at rates much greater than are typical for catalysis, a suggestion that may explain the lack of an obvious correlation between the reduction potential and position of relay stations in many intermolecular electron transfer chains. However, other experiments suggest that relay center oxidation state is not entirely innocent in the definition of catalytic rate. Resolution of oxidoreductase activity across the electrochemical potential domain by catalytic protein film voltammetry (PFV), in particular, has revealed that certain relays also act as redox switches.[2−7] Reduction of these centers can accelerate or attenuate catalysis, but the mechanisms inducing such effects have remained elusive. We previously reported that the nitrite-limited catalytic rate of a cytochrome *c* nitrite reductase operating at pH 7 was attenuated by reduction of a heme-based relay.[5−7] Here we show that this center acts as a switch only when its reduction is uncoupled from proton transfer.

Escherichia coli cytochrome *c* nitrite reductase crystallizes as a homodimer containing 10 c-type hemes.[8] It belongs to a group of homologous enzymes that catalyze the reduction of nitrite to ammonium.[9] PFV in 1 μM nitrite with an electrode rotated at 3000 rpm reveals an activity-potential profile for nitrite-limited reduction that is independent of the scan direction and that has strong pH dependence (Figure 1). At pH 8, maximal reductive (negative) catalytic current appears only in a narrow window of potential. Approximately 60% of this activity is lost on taking the film from −0.22 to −0.50 V despite application of an increased driving force for the reaction being catalyzed. This behavior, observed in reverse on returning to more positive potentials, was termed the "tunnel-diode" effect when it was first observed in a succinate-dehydrogenase.[10] By contrast, reduction of the nitrite reductase at pH 4 produces a sigmoidal increase of activity with the maximal catalytic current sustained below −0.2 V. Transferring the film between solutions of distinct pH shows that the effects of pH are fully reversible. Thus, the activity-potential profile of cytochrome *c* nitrite reductase is transformed between that of "tunnel-diode" and "diode" simply by a change of pH.[11]

Voltammetry at pH ≥ 8 was independent of electrode rotation rate above 1000 rpm and is thus free from mass-transport limitation. At more acidic pH, the film has greater activity (vide infra). Here voltammograms were never completely independent of rotation rate. However, even at pH 4, the rotation rate dependence of key voltammetric features indicates that properties determined at 3000 rpm are expected to differ from those at infinitely high rotation rates by less than 15 mV. Thus, we consider that the voltammograms at 3000 rpm provide a good reflection of steady-state behavior across the pH range studied.

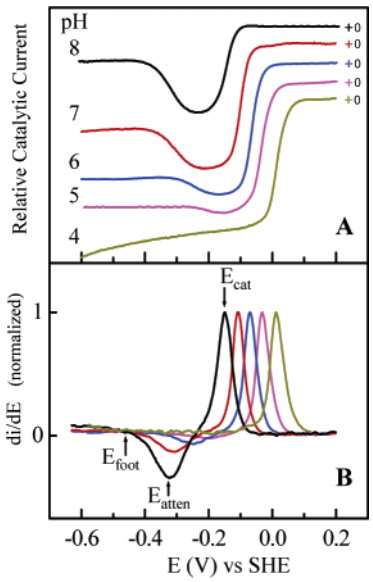

Figure 1. Representative PFV of *E. coli* cytochrome *c* nitrite reductase in 1 μM NO_2^- at the pH indicated. (A) Catalytic current−potential profiles. Each profile was recorded with a separate film, and the magnitude was normalized to that recorded in 1 μM nitrite, pH 7, to remove the effects of film-to-film variation in catalytic magnitude. (B) First derivatives of the catalytic currents in A with respect to applied potential normalized to the height of the positive peak. The positions of E_{cat}, E_{atten}, and E_{foot} are illustrated for the pH 8 data set. Measurement conditions: temperature 25 °C, scan rate 30 mV s^{-1}.

Overlaid plots of the first derivatives of catalytic current with respect to applied potential highlight their pH-dependent features (Figure 1B). The positive peak describes the increase of activity observed on lowering the potential sufficiently to reduce the enzyme to a state competent in nitrite reduction. The half-height width (52 ± 5 mV) is indicative of a coordinated $2e^-$ process at each pH, and the peak potential (E_{cat}) is displaced −38 mV per pH unit (Figure 2). Thus, nitrite reductase activity is turned on by a coordinated $2e^-$ reduction of the enzyme that is coupled to a single protonation event. That the E_{cat} versus pH plot shows no deviations from linearity indicates that the proton binds to a site with pK_a > 8.5 when the $2e^-$ center is reduced and pK_a < 4 when the $2e^-$ center is oxidized.

Under the experimental conditions, with the NO_2^- concentration well below the Michaelis constant at each pH, the enzyme sees substrate only occasionally. The electrode potential defines oxidation state, and modulations of activity are most simply interpreted as Nernstian titration of those centers whose oxidation state influences enzyme activity.[5,7] In agreement with this proposal, the value of E_{cat} at pH 7 correlates with the midpoint potential of the

10.1021/ja054160s CCC: $30.25

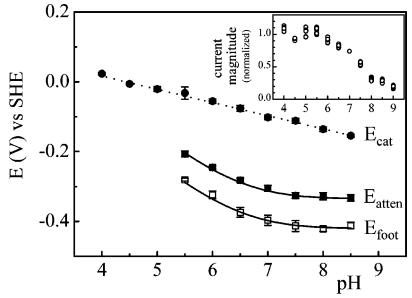

Figure 2. The pH dependence of features in the steady-state catalytic current−potential profiles from *E. coli* cytochrome *c* nitrite reductase in 1 μM nitrite. E_{cat}, E_{atten}, and E_{foot} are defined in Figure 1B. Broken line: linear fit to E_{cat} with gradient −38 mV per pH unit. Solid lines: fit to model for 1e$^-$ reduction coupled to two protonation events with p$K_a^1 = 7.1$, p$K_a^2 = 6.0$, where $E_{atten} = -335$ mV and $E_{foot} = -420$ mV in the alkaline limit.[12] Inset: pH variation of the catalytic current magnitude at −0.6 V normalized to the average of the pH 5 data points.

pair of spin-coupled hemes ($E_{m,7} \sim -107$ mV) defined by EPR spectroscopy and potentiometric titration.[7] This pair incorporates a bis-histidine-coordinated heme and its neighbor that has axial ligands of lysine and $H_2O(OH^-)$, with the latter displaced by nitrite during catalysis. Protonation of a porphyrin propionate or the side chains of Tyr216, Arg106, or His264 found on the distal face of the lysine-coordinated heme may be coupled to reduction of this heme pair to facilitate nitrite reduction.

Where further reduction of the enzyme results in attenuation of activity, a negative feature appears in the catalytic current derivatives (Figure 1B). That the potentials at the peak (E_{atten}) and foot (E_{foot}) of this feature show the same pH dependence argues that the feature is not significantly convoluted with changes in activity at higher potentials for any pH. When the negative feature is well defined, its half-height width (93 ± 18 mV) is indicative of a 1e$^-$ transformation. The variation of E_{atten} and E_{foot} is then described by a model in which 1e$^-$ reduction is accompanied by two, independent protonation events with pK_a values of 7.1 ± 0.2 and 6.0 ± 0.3 (Figure 2).[12] Thus, at pH ∼ 8, where the "low" potential reduction occurs without accompanying protonation(s), attenuation of nitrite reductase activity is most pronounced. On moving to more acidic pH, this reduction is increasingly coupled to protonation(s), and the extent of attenuation decreases until it is no longer detectable at pH 4.

At pH 7, the attenuation is centered on a potential (E_{atten}) of −300 ± 20 mV. Again, this correlates with the results from potentiometric studies and the midpoint potential ($E_{m,7} \sim -323$ mV) of the heme(s) giving rise to a large *g*-max signal and whose reduction leads to EPR silent and presumably fully reduced enzyme.[7] Large *g*-max signals arise from bis-histidine-coordinated hemes whose imidazole rings take an approximately perpendicular configuration and there are two such hemes in nitrite reductase. They form a plausible electron transfer chain between the pair of spin-coupled hemes and a region on the enzyme surface that may facilitate intradimer electron exchange and/or intermolecular electron exchange with the physiological redox partner, NrfB. An accumulation of uncompensated negative charge in this area of the enzyme is clearly detrimental to catalysis. Sites where protonation may negate this effect include the propionates of the low potential heme(s) and the side chains of His388 and His391 that lie in the vicinity of these hemes.

Our proposal that protonation coupled to reduction of a heme-based redox switch is a direct determinant of enzyme activity is supported by the pH dependence of the catalytic current at −0.6 V (Figure 2 insert). The relative errors across the data set preclude an unambiguous fit to the data and reflect the less robust films that resulted from exposure to pH ≤ 5 in the film transfer experiments used to generate the data. Nevertheless, the decrease in activity between pH ∼5.5 and ∼8.5 is clear and in line with the more quantitative description of the consequences of protonation afforded by the pH dependence of E_{atten} (and E_{foot}).

Proton coupled electron transfer (PCET) is a feature of many proteins and one that underpins proton translocation in enzymes essential for biological energy transduction.[13] The chemistries underlying such systems are beginning to emerge, but correlating individual PCET events with their catalytic consequences remains a considerable experimental challenge. Simultaneous definition of activity in the potential and pH domains by PFV has allowed us to present such data here for a multi-centered oxidoreductase. It is clear that PCET at redox centers remote from, and intimately associated with, the nitrite-binding site play important roles in determining the activity of the enzyme. With respect to the attenuation at lower potentials, it seems unlikely that changes in the reduction potential of a relay could give rise to the observed effects.[1] It is also difficult to see how significant changes in heme spacing can be accommodated within the enzyme. Thus, we favor redox driven conformational change as the mechanism responsible for the rate attenuation as manifest through a change in reorganization energy associated with ET or the rate of a chemical event associated with nitrite reduction. Both possibilities could explain why the attenuation is less pronounced at higher nitrite concentrations.[5] Under these conditions of increased electron flux, electrons may not reside on the relay for sufficient time to permit the change in conformation that would otherwise attenuate the catalytic rate. Crystallographic studies and site-specific mutagenesis in combination with PFV are now planned to resolve the molecular details behind PCET and the regulation of activity in this key N-cycle enzyme.

Acknowledgment. We are grateful to David Moore for preliminary experiments, to Dr. Christine Moore for protein purification, and for funding from BBSRC (B18695, B17233), EPSRC (DTA award to J.D.G.), and a JIF award (062178).

Supporting Information Available: Experimental methods, further analysis of voltammograms, an illustration of nitrite reductase highlighting the features discussed (PDF). This material is available free of charge via the Internet at http://pubs.acs.org.

References

(1) Page, C. C.; Moser, C. C.; Dutton, P. L. *Curr. Opin. Chem. Biol.* **2003**, *7*, 551−556.
(2) Butt, J. N.; Thornton, J.; Richardson, D. J.; Dobbin, P. S. *Biophys. J.* **2000**, *76*, 1001−1009.
(3) Léger, C.; Elliot, S. J.; Hoke, K. R.; Jeuken, L. J. C.; Jones, A. K.; Armstrong, F. A. *Biochemistry* **2003**, *42*, 8653−8662.
(4) Armstrong, F. A. *Curr. Opin. Chem. Biol.* **2005**, *9*, 110−117.
(5) Angove, H. A.; Cole, J. A.; Richardson, D. J.; Butt, J. N. *J. Biol. Chem.* **2002**, *277*, 23374−23381.
(6) Gwyer, J. D.; Richardson, D. J.; Butt, J. N. *Biochemistry* **2004**, *43*, 15086−15094.
(7) Butt, J. N. *Rec. Res. Dev. Biochem.* **2003**, *4*, 159−180.
(8) Bamford, V. A.; Angove, H. A.; Seward, H. E.; Thomson, A. J.; Cole, J. A.; Butt, J. N.; Hemmings, A. M.; Richardson, D. J. *Biochemistry* **2002**, *41*, 2921−2931.
(9) Simon, J. *FEMS Microbiol. Rev.* **2002**, *26*, 285−309.
(10) Sucheta, A.; Ackrell, B. A. C.; Cochran, B.; Armstrong, F. A. *Nature* **1992**, *356*, 361−362.
(11) This analogy is made due to the similar current−potential characteristics of the systems. To date, PFV has failed to detect catalytic oxidation by nitrite reductase. Thus, net current flow through the enzyme appears unidirectional, and diodes show a similar propensity to support substantial currents in one direction only. Tunnel−diodes show a region of negative resistance to this flow of current, as seen in the current−profile of nitrite reductase at pH 8 but not at pH 4. Streetman, B. G. *Solid State Electronic Devices*, 2nd ed.; Prentice-Hall: New Jersey, 1980.
(12) Zu, Y.; Fee, J. A.; Hirst, J. *J. Am. Chem. Soc.* **2001**, *123*, 9906−9907. Equation 1 with K_{ox1} and $K_{ox2} \gg a_{H+}$.
(13) Brzezinski, P. *TIBS* **2004**, *29*, 380−387.

JA054160S